ELSEVIER

Electroencephalography and clinical Neurophysiology 102 (1997) 452–459

A systematic evaluation of the spherical model accuracy in EEG dipole localization

B. Yvert*, O. Bertrand*, M. Thévenet, J.F. Echallier, J. Pernier

Brain Signals and Processes Laboratory, INSERM U280, Lyon, France

Accepted for publication: 16 December 1996

Abstract

This paper presents a study of the intrinsic localization error bias due to the use of a spherical geometry model on EEG simulated data obtained from realistically shaped models. About 2000 dipoles were randomly chosen on the segmented cortex surface of a particular subject. Forward calculations were performed using a uniformly meshed model for each dipole located at a depth greater than 20 mm below the brain surface, and locally refined models were used for shallower dipoles. Inverse calculations were performed using four different spherical models and another uniformly meshed model. It was found that the best spherical model lead to localization errors of 5–6 mm in the upper part of the head, and of 15–25 mm in the lower part. The influence of the number of electrodes upon this intrinsic bias was also studied. It was found that using 32 electrodes instead of 19 improves the localization by 2.7 mm on average, while using 63 instead of 32 electrodes lead to improvements of less than 1 mm. Finally, simulations involving two simultaneously active dipoles (one in the vicinity of each auditory cortex) show localization errors increasing by about 2–3 mm. © 1997 Elsevier Science Ireland Ltd.

Keywords: Realistic head models; Spherical head model; Local refinement; Boundary element method; Inverse problem accuracy

1. Introduction

Despite its very rough approximation of the head geometry, the spherical model has been providing a powerful tool to address clinical and physiological questions concerning the source locations of brain electrical activities using either EEG or MEG signals. However, the evaluation of the localization accuracy that it provides has been very seldom carried out with EEG data.

In MEG studies, several evaluations of the spherical model accuracy using physical phantoms (either spherical phantoms or skulls filled with saline water) or intracranial stimulations in epileptic patients have been carried out. Considering a small number dipoles, they have reported localization errors ranging from 2–3 mm for saline sphere phantoms and up to 8–10 mm for skull phantoms or intracranial (Barth et al., 1986; Weinberg et al., 1986; Yamamoto et al., 1988; Cohen and Cuffin, 1991). A few MEG simulations, using non-spherical head shape to perform the forward problem and a spherical model to solve the inverse problem, also reported inaccuracies ranging from 4 to 10mm (Meijs et al., 1988; Cuffin, 1990).

To our knowledge, the first evaluation of the spherical model accuracy in real EEG situations was using activation of intracerebral electrodes in epileptic patients (Cuffin et al., 1991). The authors simulated 28 dipoles in three subjects and, using 16 scalp electrodes, found the localization accuracy to be 11 mm on average, with a maximum of 25.7 mm. However, this study could obviously not cover the entire brain volume, and the electrode locations were chosen in the vicinity of the dipoles, which would not apply in practical situations where no a priori assumptions can always be made on the source locations. Recently, Cuffin (1996) used the same data set for testing the precision of realistic head models. These models were obtained by deforming a standard spherical mesh so that it fit the actual scalp shape in the upper part of the head for each subject, the skull thickness remaining constant. The author found various localization errors (ranging from 1.1 mm to 17.3 mm) depending on the position of the dipole within the head and the corresponding signal-to-noise ratio (SNR).

* Corresponding authors. INSERM - Unité 280, 151 Cours Albert Thomas, F-69003 Lyon, France. Tel.: +33 72 681901; fax: +33 72 681902.

PII S0921-884X(97)96611-X

A still growing interest has been dedicated to realistic head geometries for solving the forward and inverse problems in both EEG and MEG situations. Several evaluations of their accuracy, mostly dealing with the boundary element method, were carried out using uniformly meshed models (Roth et al., 1993; Menninghaus et al., 1994) or locally refined models (Cuffin, 1990; Bertrand et al., 1991; Yvert et al., 1995, 1996; Zanow and Peters, 1995). This offers a means for addressing in a systematic way the question of the accuracy of the spherical model accuracy by computing the forward solutions using realistic geometries.

Such a strategy was used in a few EEG studies (Cuffin, 1990; Roth et al., 1993; Zanow and Peters, 1995). However, only a small number of dipoles were considered in these studies (namely of the order of 10). Using one dipole location and six different ellipsoidal models to perform forward calculations, and a spherical model for inverse calculations, Cuffin found localization errors of less than 10 mm. Roth et al. considered eight dipole locations in both left frontal and left temporal lobe regions. They used a uniformly meshed model having 1600 elements per surface (density of 1.7 triangles/cm^2) to perform forward calculations at 21 electrode locations, and found an average localization error of 2 cm. Zanow and Peters considered two dipoles in the upper left hemisphere at two different depths (5 and 23 mm), and used 52 electrodes all placed on the very upper part of the head. Using a spherical model that best fit all electrodes, they found localization errors of 4.5–6.5 mm in the absence of noise, and 5.7–10.6 mm when additional gaussian noise (SNR = 10, 20) was considered.

The following EEG study aims at systematically evaluating the intrinsic localization error bias that stems from the use of a spherical geometry model on simulated data obtained from realistically shaped models. About 2000 dipoles were randomly chosen on the segmented cortical surface of a particular subject, obtained from MR images. For each dipole, the EEG forward solution was computed with a realistic head boundary element model being locally refined near shallow sources in order to ensure a good numerical accuracy (Yvert et al., 1995). Then, inverse calculations were performed for each dipole using four different spherical models and also one uniformly meshed realistic head model. The influence of the number of electrodes on the spherical model accuracy was also studied. Similar evaluations were investigated for two dipoles located in the vicinity of both primary auditory cortices.

2. Methods

2.1. Choice of the dipole sites

In order to systematically study the behavior of the spherical model accuracy with respect to the dipole location within the brain, we considered 2000 dipoles located on the outer white matter surface of a particular subject which initially constituted 224 000 points. This surface (Fig. 1) was obtained using a region growing algorithm working on gray levels of the images corresponding to the white matter (Fuchs et al., 1994). Dipole orientations were taken perpendicular to the surface. In order to be able to superimpose the localization errors over MR images, dipoles were randomly chosen on 10 horizontal slices (labeled 1 to 10) separated by 10 mm, going from the top of the head down to the lower tip of the temporal lobes (Fig. 1). In each slice, the distance between two neighboring dipoles was about 5 mm.

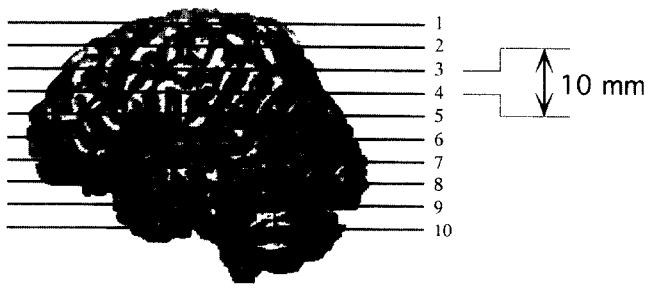

Fig. 1. Cortical surface extracted from MR images. Dipoles are randomly chosen on the intersection of this surface with 10 horizontal plane. Their moment orientations are perpendicular to the local surface. The distance between two neighbor dipoles within each slice is about 5 mm.

2.2. Forward models

In a previous study (Yvert et al., 1995), we explicitly proposed strategies for choosing appropriate mesh element densities to improve the accuracy of forward EEG calculations. It was shown that for dipoles located at more than 20 mm from the brain envelope, a uniformly meshed model could be used, whereas for shallower sources, meshes should be locally refined. According to these results and also to those obtained in evaluating the inverse problem accuracy in spherical and realistic geometries (Yvert et al., 1996), we found that the locally refined area should be of radius 30 mm over the dipole site.

For these reasons, we considered two different types of forward three-shell models (Fig. 2). For deep dipoles (depth > 20 mm), we used a uniformly meshed model (called forward uniformly meshed model (FUMM)) having 4000 triangles and a global mesh density of 1.3 triangles/cm^2, whereas for shallow dipoles we used locally refined models with a global mesh density of 0.8 triangles/cm^2 and a local mesh density of 10 triangles/cm^2. In order to cover all shallow dipole sites, it was necessary to build 51 different locally refined models, 2 of which are shown in Fig. 2. The meshing methods have already been detailed in our previous papers (Yvert et al., 1995, 1996).

The boundary element method considered the potential to be constant on each triangle, and as suggested by Hämäläinen and Sarvas (1989) and by Meijs et al. (1989), the isolated problem approach was used. Because the FUMM was used for more than 500 dipoles, a LU decomposition of the

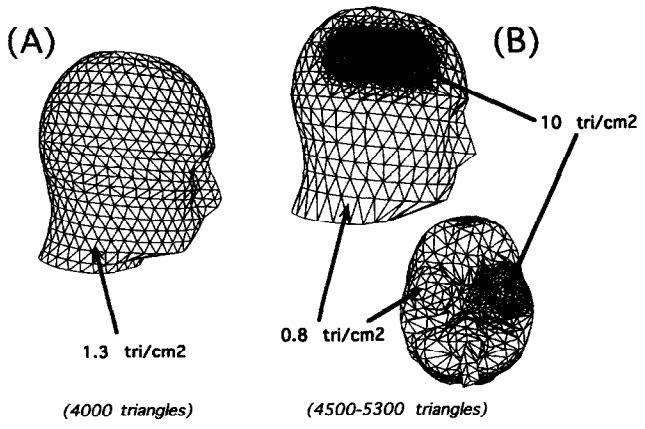

Fig. 2. BEM models used to compute the forward solutions. (A) The FUMM (scalp shell), which was used for deep dipoles. (B) Two examples of locally refined models used for shallow dipoles; one scalp shell refined in the right temporal region, and one brain shell with a refinement of the left temporal lobe.

deflated matrix was computed in this case, which provided fast forward calculations. However, because only a few dipoles were concerned by each of the locally refined models, it was faster to use iterative resolutions (Gauss–Seidel method) in these cases. The conductivities of the brain, skull, and scalp were 0.45, 0.05625, and 0.45 Siemens/m, respectively, according to Rush and Driscoll (1969). Forward solutions were computed at 63 electrodes of the extended 10–20 system, that were placed on each model (Fig. 3).

2.3. Inverse models

Four different analytical spherical models were used to solve the inverse problems. Their normalized radii for the scalp, skull, and brain layers were 1, 0.92, and 0.87,respectively. Their conductivities were the same as those of the forward models. Each model has the following characteristics, which could be inferred only from the electrode positions.

Model 1: Spherical model having its center roughly at the intersection of FPz-Oz and T3-T4 electrodes (Echallier et al., 1992), and whose external radius was the mean of all electrode radial coordinates.

Model 2: Spherical model that best fit all electrodes locations in a least square sense.

Model 3: 'Multi-radius' spherical model having the same center as that of Model 2 and whose external radius was, for each electrode, the radial coordinate of the electrode.

Model 4: Same model as Model 2, except that the position of each estimated dipole found to be at (r,θ,φ), in common spherical coordinates with Model 2, was radially corrected as follows. At the same angle coordinates (θ,φ), the radius R_s of the spherical spline (Perrin et al., 1989) passing through all electrode locations was computed. The dipole radial coordinate r was then multiplied by the ratio of R_s over the external radius of Model 2.

Electrodes placed on the forward models were radially projected on each spherical model. Inverse calculations were also performed using a uniformly meshed model (called inverse uniformly meshed model (IUMM)) having the same global density as that of the FUMM (1.3 triangles/cm^2), and the same number of triangles (4000). The IUMM was derived from the FUMM by randomly swapping 1000 edges of each layer of the latter so that both remained geometrically identical, while becoming numerically different. Although the accuracy of such a model has already been addressed in a previous study (Yvert et al., 1996), this complementary result would be more easily paralleled to those obtained with the various spherical models.

2.4. Initial conditions for the inverse procedure

The inverse problem was solved by a mixed linear/nonlinear (Marquardt) algorithm. It has been observed that the

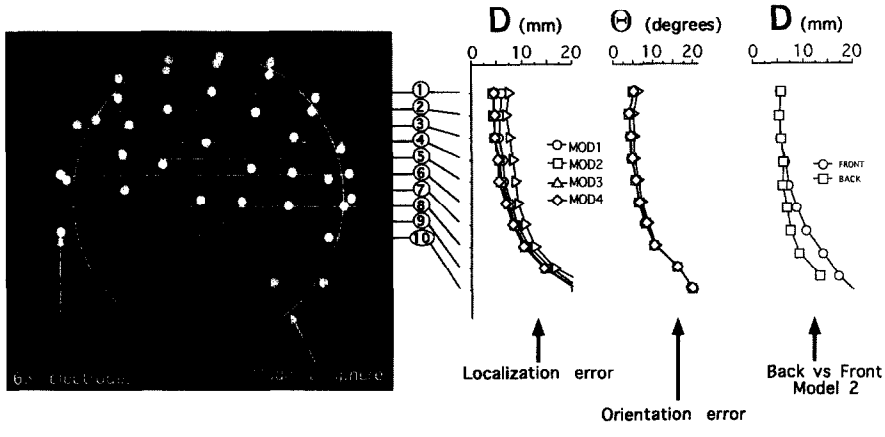

Fig. 3. The localization and orientation errors (D and Θ, respectively) obtained with the four spherical models are averaged over all dipoles in each slice. It appears that they become greater in the lower part of the head with respect to the upper part. The diagram on the far right shows localization errors obtained with Model 2 (the best spherical model), for dipoles situated both forward with respect to the plane (T3, T4, Cz) and backward. It shows that errors are greater in the front of the head.

choice of the initial condition of this inverse process may affect the solution. For this reason, when spherical models were considered, 30 inverse calculations with random initial conditions were performed, and the calculation leading to the lowest mean-square difference between the actual electrode values and the estimated ones was retained. When the IUMM was used for inverse calculations, the realistic inverse process was initialized with the solution of the spherical Model 1. When Model 1 found dipoles outside the inner shell of the IUMM, the radial coordinate of the dipole was iteratively multiplied by 0.9 until it laid within the inner shell of the IUMM.

3. Results

3.1. Comparison between the different spherical models

In this section, 63 electrodes were used, and all four spherical models were compared. Localization and orientation errors averaged in each slice are shown in Fig. 3 together with the projection of the electrode locations on a sagittal MR image.

We compared the accuracy of the four different models using the non parametric Quade test, followed by the a posteriori Conover 2×2 comparison (Conover, 1980) between all pairs of models. This test is equivalent to the classical parametric one-way ANOVA with post-hoc test using the Bonferroni correction. However, it does not assume normally distributed data.

It appeared that localization errors significantly depended on the choice of the model ($P < 0.0001$). More precisely, Model 4 was better than Models 1 and 3 ($P < 0.0001$), Model 4 was better than Model 2 ($P < 0.013$) and Model 2 was better than Models 1 and 3 ($P < 0.0001$). However, the average localization error difference between Models 2 and 4 was less than 0.5 mm, and furthermore, if slices 4 and 5 were not taken into account, errors between Models 2 and 4 were no longer significantly different ($P = 0.088$). For these reasons, only Model 2 has been considered in the following.

It turns out that, for all models, errors are smaller in the upper part of the head (4–6 mm, 4–7°) than in the lower part (15–25 mm, 10–20°). Furthermore, in the lower part of the head, localization is significantly better in the posterior part of the head (posterior to the plane T3-Cz-T4) than in the anterior part (7–15mm versus 10–20mm). Fig. 4 shows localization errors obtained for Model 2 as color coded plots over MRIs.

Finally, it was noted that dipoles oriented rather vertically were found to be too anterior (3 mm on average), whereas dipoles oriented rather horizontally were found to be too

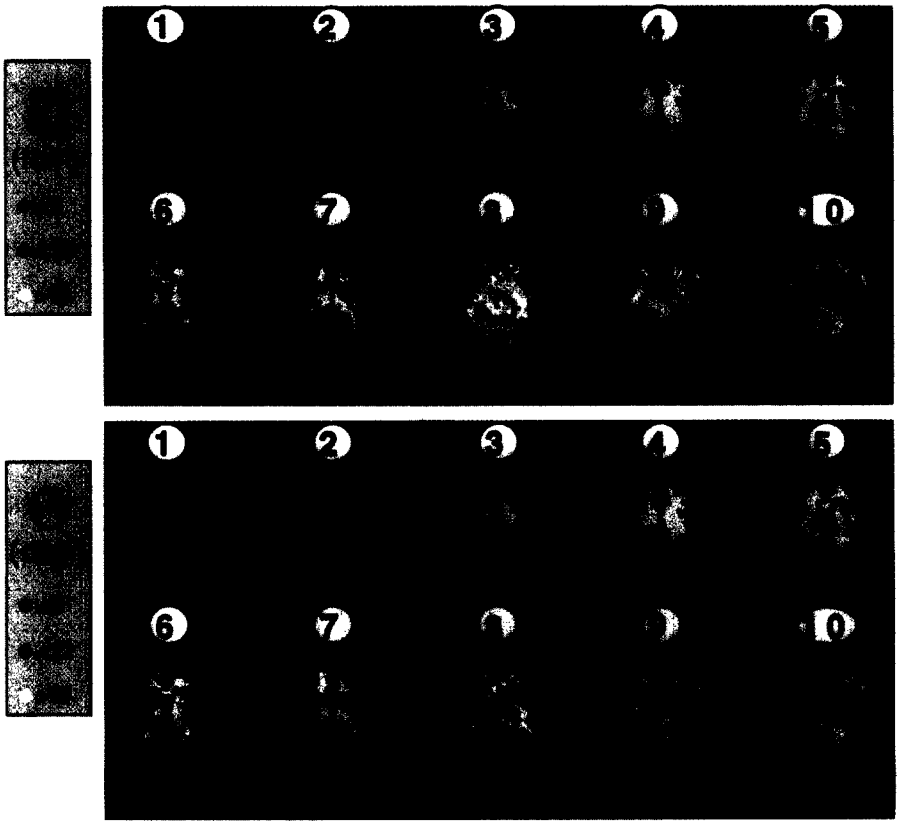

Fig. 4. Color map of the localization (D in mm) and orientation (Θ in degrees) errors obtained with the best spherical model (Model 2) for all dipoles of all slices. Each location is plotted in red if the error at that position is less than 6 mm or 6°, in blue if it is between 6 mm and 12°, and in yellow if it is more than 12 mm or 12°.

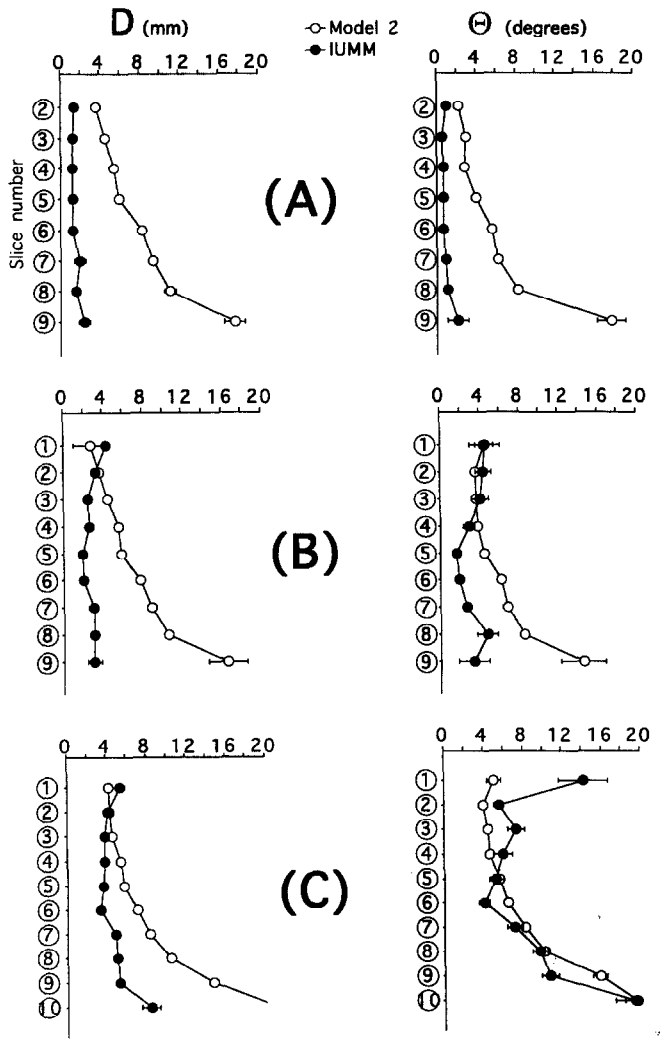

Fig. 5. Localization and orientation errors (D and Θ, respectively) obtained with both the IUMM and Model 2. Three cases are considered; (A) only deep dipoles (depth>20 mm) are taken into account, (B) dipoles with depth>15 mm are introduced, and (C) all dipoles are considered. Note that there is no dipole with depth>15 mm in slice 10.

high up (5 mm on average) especially in the lower part of the head, and too much anterior (3 mm on average).

3.2. Comparison between the spherical Model 2 and the IUMM

Localization and orientation errors obtained using Model 2 and the IUMM are reported in Fig. 5. Three cases are separately presented. First (Fig. 5A), only deep dipoles (depth > 20 mm) are considered, next (Fig. 5B), shallower dipoles having a depth > 15 mm are considered, and finally (Fig. 5C) all dipoles are taken into account.

Using Model 2, not much difference appears from one case to the next for both types of errors. Using the IUMM, dipole locations and orientations are found with an average accuracy of 1.4 mm and 0.7° in the first case, 2.5 mm and 3° in the second case, and 4.4 mm and 7.6° in the third case. In the first two cases, errors obtained with the IUMM did not vary much from one slice to the other. In the third case, both types of errors, and especially the orientation errors, become greater in the lower part of the head. Localization errors still remain much lower than those obtained with Model 2, whereas orientation errors become comparable. These later errors were also found to be greater in slice 1, where a majority of dipoles were very shallow (depth < 15 mm).

3.3. Influence of the number of electrodes

In a separate study, three different montages were considered, having 19, 32, and 63 electrodes, respectively. Model 2 was used to perform inverse calculations. Results, together with the electrode locations projected on the anatomy of the subject (sagittal MRIs) are presented in Fig. 6.

It appears that using 32 electrodes rather than 19 decreases the localization error bias of Model 2 in the upper part of the head by 3 mm. Improvement in the lower part of the head can be achieved using 63 electrodes (a reduction of 1 mm). By contrast, no such differences are observed for the orientation errors.

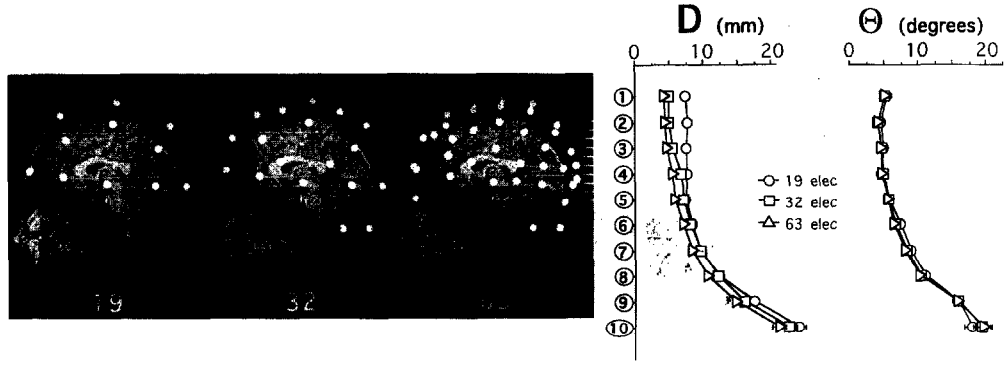

Fig. 6. Effect of the number of electrodes on the localization and orientation errors (D and Θ, respectively) obtained with Model 2. Three electrode arrangements are considered (19, 32 and 63), and for each, electrodes are projected onto a sagittal MRI.

3.4. Two dipole results

The precision of the spherical model was also studied in the case of two simultaneously active dipoles, each one located in the vicinity of the primary auditory cortices. One hundred pairs of such bilateral dipoles were randomly chosen (Fig. 7B). Inverse calculations were performed with 63 electrodes, using both Model 2 and the IUMM. Localization and orientation errors in both cases are shown in Fig. 7A, for deep dipoles (depth > 20 mm) on one hand and for all dipoles on the other hand. For deep dipoles, the average localization error is 10.4 mm for Model 2 and 5.7 mm for the IUMM, and the orientation errors are 10.7° and 7.1°, respectively. As in the case of one dipole, when shallow dipoles are taken into account, errors (and especially the orientation error) become greater for the IUMM (8.2 mm and 12.6°), whereas they vary much less for Model 2 (11.2 mm and 11.5°).

The right and left localization and orientation errors were not significantly different using a non parametric Mann–Whitney test (which does not assume the normality of the data) for both Model 2 ($P = 0.85$ for the localization error, and $P = 0.47$ for the orientation error) and the IUMM ($P = 0.31$ for the localization error, and $P = 0.63$ for the orientation error).

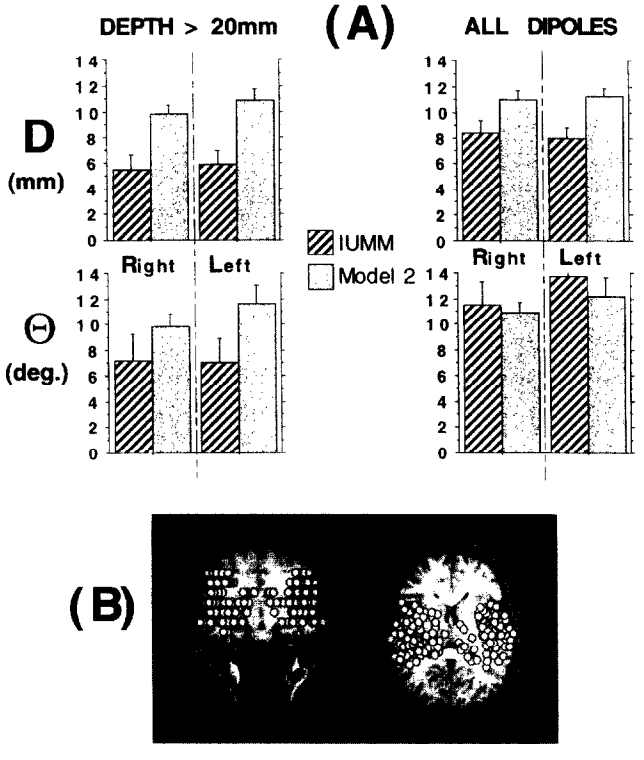

Fig. 7. Two dipole results. (A) Localization and orientation errors obtained for both left and right dipoles with Model 2 and the IUMM. (B) Dipole locations projected on two orthogonal MRIs. The apparent differences between left and right dipoles were not found to be significant using a non parametric Mann–Whitney test.

4. Discussion

In order to evaluate the level of the intrinsic error bias of the spherical model, our results have to be paralleled with inverse calculation errors obtained with realistic head models. Our simulations performed with the IUMM and dipoles located at a depth > 15 mm show intrinsic errors of realistic models of the order of 2–3 mm. This is consistent with previously reported studies (Roth et al., 1993; Yvert et al., 1996).

Our results for one dipole show an average localization error of the order of 10 mm with a spherical model, which agrees with results found with few dipoles by other authors (Cuffin et al., 1991; Roth et al., 1993; Zanow and Peters, 1995). However, from the present study, it clearly appears that the localization accuracy greatly depends upon the dipole location within the brain. In particular, it is relatively good in the upper part of the head (4–5 mm) and much worse in the lower part of the head (15–25 mm). Orientation errors have a comparable behavior: 4–6° in the upper part and 10–20° in the lower part. At first sight, high errors in the lower part of the head may be explained by two different reasons; firstly by the lack of electrodes below T3, T4, FPz and Oz, and secondly by the non-spherical shape of the head structures (brain, skull and scalp) in this region. However, results reported in Fig. 4 using the IUMM clearly reveal that the second reason is the main cause of errors. Indeed in cases A and B, errors obtained with the IUMM appear not to vary from the upper to the lower part of the head, whereas they do dramatically increase for Model 2. This advocates that the lack of electrodes in the lower part of the head is far less a cause of error for Model 2 than the non sphericity of the head. This point is emphasized by the fact that using more electrodes does not much improve the localization accuracy in the lower part of the head.

In case C, where shallow dipoles (depth < 15 mm) are also taken into account, errors obtained with the IUMM, and especially the orientation errors, increase. This agrees with our previously reported results on the intrinsic errors obtained with realistic models (Yvert et al., 1996), and is due to the fact that the IUMM is uniformly meshed and not locally refined. It is to be noted that because there are higher proportions of shallow dipoles in slices 1 and 8–10 than in the other slices, average errors are found to be higher in these slices.

Although we considered only cortical dipoles, some were very deep in the brain (such as in the interhemispheric fissure). We observed that for dipole depths greater than 40 mm, average localization errors obtained with Model 2 varied from 5 mm on slice 5 to 15 mm on slice 8. Thus, localization errors for dipoles located in deep structures (e.g. in thalamus nuclei), will very likely depend on the position of the structure within the brain (upper or lower part).

Our results can be compared to those of Roth et al. (1993). In their study, they found an average localization error of approximately 20 mm for the spherical model,

which is slightly higher than our findings. However, this value is an average over 24 dipoles, and half of them were located quite low in the left temporal lobe. Indeed, the average localization error for their frontal dipoles is 13.7 mm, whereas it is 25.6 mm for their temporal dipoles. They also evaluated the intrinsic error of their 1600 element uniformly meshed realistic model to be 4.8 mm. This is consistent with our results when all dipoles are taken into account (we found 4.4 mm in this case). However, when only deep dipoles are considered, this intrinsic error is reduced to 1.4 mm. Hence the differences between their results and ours are very likely due to the fact that some of their dipoles were quite shallow and they used only a uniformly meshed model to perform all forward problems. It is also interesting to note that their results for horizontally oriented dipoles differ from those obtained for vertically oriented dipoles in a very similar way as in our simulations. In their study, horizontal dipoles are found to be too high and anterior, whereas vertical dipoles are found to be too low and anterior.

Our results concerning the influence of the number of electrodes on the spherical model bias show that improvements (about 2–3 mm) are evident when using 32 electrodes instead of 19, especially in the upper part of the head where the geometry is much closer to sphericity than in the lower part. However, using 63 electrodes rather than 32 improves the localization accuracy by less than 1 mm on average.

However, these results were obtained on noiseless simulated data, and might well be different in the case of noisy data. A previous work by Mosher et al. (1993) in spherical geometries addressed the question of the influence of the number of electrodes on the localization precision when using noisy data. They showed that while errors in the vicinity of the electrode array could be of the order of 20–30 mm with the usual 21 electrodes of the 10–20 system, they could be reduced to 4–10 mm using 37 electrodes, and to 2–5 mm using 127 electrodes. However, their study assumed that no systematic error was made due to the model geometry (the same four-shell spherical model was used to simulate data and solve the inverse problem), and that the localization errors were only due to noise. By contrast, our study concerned systematic errors relative to the choice of geometrical model. While increasing the number of electrodes reduces the localization error with noisy simulated data in spherical head shape (Mosher et al., 1993), our results show that a systematic error remains despite the use of additional electrodes, due to the inadequacy of the model geometry. However, this study should certainly be extended to the case of noisy data, where the effect of an increasing number of electrodes might be more important. Indeed, Cuffin (1996) suggested that realistic models give in general lower errors than spherical models for high SNR. However, in studies using intracranially generated dipoles, the dipole position within the head is strongly correlated to the SNR, and sometimes it may be difficult to disclose the respective effects of both factors. Noisy simulations, which should be handled in a systematic manner (large number of dipoles, various SNR values) would thus be addressed in a future study.

Our simulations using two bilateral dipoles (one in the vicinity of each primary auditory cortex) reveal that localization and orientation errors are increased even when using the IUMM. In the case of one dipole, errors in this region were on average 8–9 mm and 6–8° (slices 6 and 7) for Model 2. In the case of two dipoles, they increase up to 11.2 mm and 11.5°. When using the IUMM, and when all dipoles are considered, localization errors are on average only 3 mm better than those obtained using Model 2. However, when only deep dipoles are considered, errors are only 5.7 mm for the IUMM and still 10.4 mm for Model 2. This strongly advocates that locally refined models should be used for localizing multiple shallow sources in order to get a genuinely improved accuracy than that provided by the spherical model. This was reported in a previous study (Yvert et al., 1996), where localization errors were more than 6 mm with a uniformly meshed model with the same density as the IUMM, while they were approximately 2–3 mm with a locally refined model having a global and a local mesh density 0.8 triangles/cm^2 (global) and 5 triangles/cm^2 (local).

Our study did not consider other multiple dipole configurations, because a great deal of situations should be explored in order to be exhaustive, which is far beyond the scope of this paper.

It should be noted that we used the center of gravity (COG) approach for the boundary element method, which assumes the potential to be constant over each triangle. In order to improve the numerical accuracy of this method, one would be tempted to use linear interpolation over each element as suggested by De Munck (1992). However, in a simulation study, Schlitt et al. (1995) reported that linear interpolation did not bring considerable improvements over the COG approach for a similar mesh size. Surprisingly, we found similar results in a preliminary study. Hence, a systematic and careful comparison of both methods would be of high practical value.

Acknowledgements

The authors wish to thank Professor J.C. Froment from the Neurological Hospital of Lyon for providing MR images. This work was supported in part by a grant from Région Rhône-Alpes (France).

References

Barth, D.S., Sutherling, W., Broffman, J. and Beatty, J. Magnetic localization of a dipolar current source implanted in a sphere and a human cranium. Electroenceph. clin. Neurophysiol., 1986, 63: 260–273.

Bertrand, O., Thévenet, M. and Perrin, F. 3D finite element method in brain electrical activity studies. In: J. Nenonen, H.M. Rajala and T.

Katila (Eds.), Biomagnetic Localization and 3D Modelling. Helsinki University of Technology, Report TKK-F-A689, 1991, pp. 154–171.

Cohen, D. and Cuffin, B.N. EEG versus MEG localization accuracy: theory and experiment. Brain Topogr., 1991, 4: 95–103.

Conover, W.J. Practical Nonparametric Statistics, 2nd edn. Wiley, New York, 1980.

Cuffin, B.N. Effects of head shape on EEGs and MEGs. IEEE Trans. Biomed. Eng., 1990, 37: 44–52.

Cuffin, B.N., Cohen, D., Yunokuchi, K., Maniewski, R., Purcell, C., Cosgrove, G.R., Ives, J., Kennedy, J. and Schomer, D. Tests of EEG localization accuracy using implanted sources in the human brain. Ann. Neurol., 1991, 29: 132–138.

Cuffin, B.N. EEG localization accuracy improvements using realistically shaped head models. IEEE Trans. Biomed. Eng., 1996, 43: 299–303.

De Munck, J.C. A linear discretization of the volume conductor boundary integral equation using analytically integrated elements. IEEE Trans. Biomed. Eng., 1992, 39: 986–990.

Echallier, J.F., Perrin, F. and Pernier, J. Computer-assisted placement of electrodes on the human head. Electroenceph. clin. Neurophysiol., 1992, 82: 160–163.

Fuchs, M., Wagner, M., Wischmann, H.-A., Ottenberg, K. and Dössel, O. Possibilities of functional brain imaging using a combination of MEG and MRT. In: C. Pantev (Ed.), Oscillatory Event-Related Brain Dynamics. Plenum Press, New York, 1994, pp. 435–457.

Hämäläinen, M.S. and Sarvas, J. Realistic conductivity geometry model of the human head for interpretation of neuromagnetic data. IEEE Trans. Biomed. Eng., 1989, 36: 165–171.

Meijs, J.W.H., ten Voorde, B.J., Peters, M.J., Stok, C.J. and Lopes da Silva, F.H. The influence of various head models on EEGs and MEGs. In: G. Pfurtscheller and F.H. Lopes da Silva (Eds.), Functional Brain Imaging. Springer-Verlag, Berlin, 1988, pp. 31–45.

Meijs, J.W.H., Weier, O.W., Peters, M.J. and van Oosterom, A. On the numerical accuracy of the boundary element method. IEEE Trans. Biomed. Eng., 1989, 36: 1038–1049.

Menninghaus, E., Lüntkenhöner, B. and Gonzalez, S.L. Localization of a dipolar source in a skull phantom: realistic versus spherical model. IEEE Trans. Biomed. Eng., 1994, 41: 986–989.

Mosher, J.C., Spencer, M.E., Leahy, R.M. and Lewis, P.L. Error bounds for EEG and MEG dipole source localization. Electroenceph. clin. Neurophysiol., 1993, 86: 303–321.

Perrin, F., Pernier, J., Bertrand, O. and Echallier, J.-F. Spherical splines for scalp potential and current density mapping. Electroenceph. clin. Neurophysiol., 1989, 72: 184–187.

Roth, B.J., Balish, M., Gorbach, A. and Sato, S. How well does a three-sphere model predict positions of dipoles in a realistically shaped head? Electroenceph. clin. Neurophysiol., 1993, 87: 175–184.

Rush, S. and Driscoll, D.A. Electrode sensitivity – an application of reciprocity. IEEE Trans. Biomed. Eng., 1969, 16: 15–22.

Schlitt, H.A., Heller, L., Aaron, R., Best, E. and Ranken, D.M. Evaluation of boundary element methods for the EEG forward problem: effect of linear interpolation. IEEE Trans. Biomed. Eng., 1995, 42: 52–58.

Weinberg, H., Brickett, P., Coolsma, F. and Baff, M. Magnetic localisation of intracranial dipoles: simulation with a physical model. Electroenceph. clin. Neurophysiol., 1986, 64: 159–170.

Yamamoto, T., Williamson, S.J., Kaufman, L., Nicholson, C. and Llinas, R. Magnetic localization of neuronal activity in the human brain. Proc. Natl. Acad. Sci. USA, 1988, 85: 8732–8736.

Yvert, B., Bertrand, O., Echallier, J.F. and Pernier, J. Improved forward EEG calculations using local mesh refinement of realistic head geometries. Electroenceph. clin. Neurophysiol., 1995, 95: 382–391.

Yvert, B., Bertrand, O., Echallier, J.F. and Pernier, J. Improvement of inverse dipole localization using local mesh refinement of realistic head geometries: an EEG simulation study. Electroenceph. clin. Neurophysiol., 1996, 99: 79–89.

Zanow, F. and Peters, M.J. Individually shaped volume conductor models of the head in EEG source localization. Med. Biol. Eng. Comput., 1995, 33: 582–588.